Practical examples of magnetic field measurements in industrial and environmental surroundings

Dr. Swen Graubner, Dr. Denis Filistovich, Dr. Stefan Hiebel, Ralf Wengerter

SEKELS GmbH,
D-61239 Ober-Moerlen, Dieselstrasse 6, Germany

Magnetic fields are present in every aspect of the human living and working environment and in a wide frequency and intensity range. Measuring these magnetic fields and evaluating them with respect to their potential to harm man and machine is an important aspect of modern EMC. Measurement and evaluation are closely connected, as most conventional magnetic field measurement devices use a filtering and summation method that relies on a sensor-integrated hardware. There is however another possible approach that is based on a separation of measurement and analysis. Advantages are a better flexibility and the possibility to use one hardware device to evaluate according to different guidelines, based on only one executed measurement. The MFA-110 is a device constructed after this philosophy. Within this publication several measurement examples for very different frequency and field strength ranges and their evaluation according to the German workers' compensation board regulation for magnetic fields BGV B11 are shown.

***Index Terms*—EMC, magnetic field, inductive heating, electric drives**

I. Introduction

Magnetic fields can be measured by several different techniques. The best known and most often used sensor types are Fluxgate-, Hall- and magnetoresistance sensors, SQUIDs and induction coils [1]. All of them have different advantages and disadvantages and different frequency and amplitude ranges. Figure 1 gives a brief overview which measurement type is suitable for which frequency range and field amplitude.

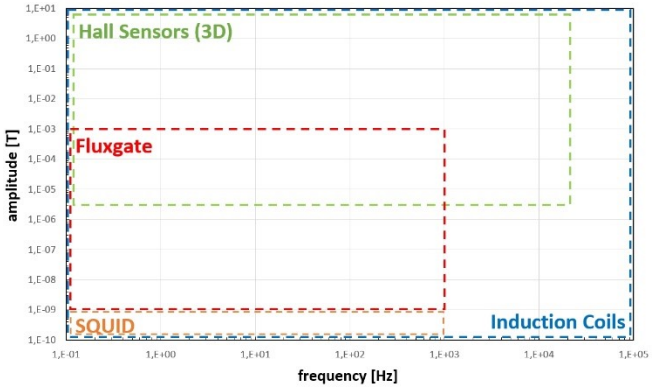

***Fig. 1: Typical m**easurement frequencies and amplitude ranges of different magnetic field measurement principles.*

SQUID sensors are by far the most sensitive detectors, but until now unable to work under room-temperature conditions and suitable only for small magnetic field strengths. This makes them a valuable sensor type for laboratory research and for some few mobile applications e. g. in geophysics [2] and bioscience [3], but difficult to use for EMC measurements.
Hall-sensors are well known as cheap and practical measurement devices. Their ability to measure over a comparably wide intensity and frequency range makes them very popular in laboratory experiments as well as for in-the-field EMC measurements. Also their small size allows precisely located measurements. However they still are limited to a maximum field frequency of around 25 kHz for 3-axis measurements [4] and are not very temperature-stable [5].
Other detector types (in particular magnetoresistance sensors) show a nonlinear field to signal behavior due to magnetic hysteresis and nonlinear saturation effects.
For AC fields very often induction coil systems are used. Changing magnetic fields induce a voltage in a coil, depending on field frequency and strength (Formula 1).

$$U_{ind} = -\frac{d\phi}{dt} = -\frac{d}{dt}\left(\int \vec{B} \cdot d\vec{A}\right)$$

***Formula 1:** Voltage induced into a conductor circuit by a magnetic field*

This signal voltage can be amplified and detected as a measure of the magnetic field strength. The measurement frequency and amplitude range can be adapted by the shape and winding geometry of the coils and the capability of the signal amplifier. Induction coil systems are not affected by hysteresis effects, as no ferromagnetic material is used in the vicinity of the coil. An orthogonal setup of three coils allows a three dimensional measurement. A disadvantage however is, that it is not possible to measure DC fields without a chopper device. Also low frequency fields need longer integration times.

Most guidelines for the protection from magnetic field contaminations demand measurements over a large frequency range [6] [7] [8] [9]. As to our best knowledge no existing device is able to measure in the full range from DC to GHz, it is common practice to use one device which is sensitive to magnetic fields and is able to measure in the low frequency range (usually up to 400 kHz), while for higher frequencies the electric field is measured by a different device.

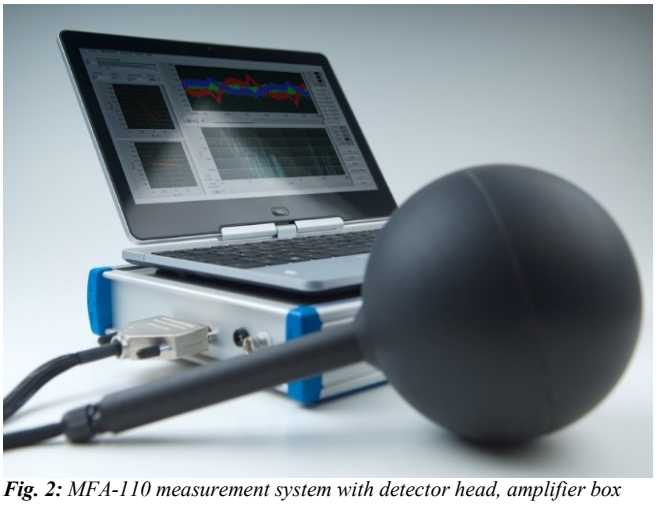

Fig. 2: *MFA-110 measurement system with detector head, amplifier box and notebook.*

This publication reports on measurements performed with an induction coil measurement system in the frequency range from 1 Hz to 400 kHz.

II. PRINCIPLES OF DATA ACQUISITION AND ANALYSIS

In guidelines for the protection against nonionizing radiation the resulting field contamination is usually not only determined by the maximum field amplitude which is detected in a certain frequency range or by a respective RMS value. Nearly all popular guidelines demand a weighted addition of all measured signals, where the frequency of the signal significantly influences its contribution to the resulting contamination value. Low-frequency fields < 50Hz usually are considered with a lower weighting factor than fields in the kHz and MHz-range, due to their increased potential to harm man and machine by the increase in the deposited power. In some guidelines specific frequencies (e.g. 50 Hz in [9]) have a higher weighting, justified by a general magnetic field "pollution" at these frequencies in the environment due to the public mains.

The realization of the measurement and weighted addition of the measured signals can be done by two different approaches:

1. *Hardware solution*: Until now the most common method is to use a detector head that already incorporates electronic circuits which apply a frequency-dependent filtering to the voltages that are induced in the detector coil. The advantage of such a system is its quick response, its relative easy to use and to analyze the results and its small amplifier and output device. However it is impossible to use the detector head for different guidelines, in particular not for guidelines which have been released after the manufacturing of the detector head. As a result of this, for every new or changed guideline a new measurement system has to be bought. Also measurement results are usually only presented in form of one percentage number, the access is very limited and post-processing often not possible.

2. *Software solution*: A new approach is to use a universal detector head that measures independently from the applied guideline. The data acquisition needs to be executed rapidly, because large amounts of data are collected during a full-frequency-range measurement. The availability of fast hard disks (like SSD) has made this approach possible. Significant advantages of the software solution are that analysis can be done later and according to several different guidelines. Also a later implementation and analysis to newly released guidelines is possible. It is also possible to use individually developed analysis methods, suited to the respective characteristics of the magnetic field. Disadvantages of software based analysis are that such systems are more complex in handling and that the amplifier and output devices are larger.

III. OVERVIEV OVER THE MFA-110 SYSTEM

The MFA-110 is an induction coil system that follows the approach Nr. 2 from the last paragraph and uses a software solution for the measurement and analysis. It has a measurement range from 1 Hz to 400 kHz and thus can take over the lower measurement range described in paragraph I. For measurements according to the most important EMC guidelines a standard detector head with a coil cross-section of 100 cm^2 is used, for other measurement tasks different detector heads are available. The sensitivity, minimum and maximum field intensity are depending on the measured frequency and are given in

Table **1**. In its standard configuration the system consists of a HP notebook with SSD hard disk, an amplifier box and the detector head. Fig. 2 shows a photography of the system, Fig. 3 a schematic sketch.

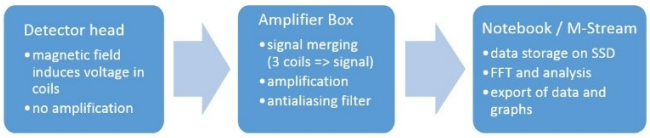

Fig. 3: *Schematic drawing of the MFA-110 measurement principle.*

Frequency [Hz]	min. field strength	max. field strength
1	6 µT	1,5 T
100	70 nT	20 mT
1000	50 nT	15 mT

Table 1*: Measurement range specifications*

IV. MAGNETIC FIELD SAFETY GUIDELINES

Protection guidelines like [6] [7] [8] [9] differ significantly from EMC guidelines, which have been conceived mostly to reduce parasitic noises in signal transmission, telecommunications, television and mobile communication. Although fields in the "classical" EMC-frequency range from MHz to GHz are electromagnetic fields as well and in principle able to harm human beings, the focus of most EMC guidelines is different, also the methods of evaluation.

Safety guidelines for electromagnetic fields have been released by multiple organizations, national as well as international. Of outstanding international importance are the publications from 1998 [7] and 2010 [6], released by the International Commission on nonionizing radiation protection (ICNIRP). ICNIRP is an

international association of scientists, supranational and acknowledged by the WHO as well as by the European Union [10]. Although the ICNIRP publications are of no judicative importance they have influenced many national guidelines.

For Germany of significant importance are the guidelines [9], which is part for the German environmental law and responsible for the general public health and safety, and [8] which governs the electromagnetic field contaminations in the industrial and working environment. In particular manufacturers and operators of industrial machines are often bound to ensure compliance with [8], while [9] is more important for household appliances, power-lines and distribution transformers.

Because of their importance in Germany these two guidelines will be discussed in more detail:

26. BImSch [9] distinguishes between low-frequency (< 9 kHz), high frequency (> 9 kHz), DC and pulsed magnetic fields. For low frequency fields maximum flux densities are given. For example at 50 Hz a magnetic flux density of 100 µT may not be surpassed. For higher frequency magnetic fields the guideline only regulates fields by devices with more than 10 W power, a rather unimportant limitation for power applications. For the whole frequency range in addition to the critical values at the respective frequencies also a summation criterion has to be fulfilled (Formula 2). $I_{M,i}$ is the magnetic field strength at the frequency band f_i , $G_{M,i}$ is the critical value at the same frequency band.

$$\sum_{1\ \mathrm{Hz}}^{10\ \mathrm{MHz}} \frac{I_{M,i}}{G_{M,i}} \leq 1$$

Formula 2: *Summation formula for magnetic fields from multiple sources in [9].*

The criterion in principle is a non-weighted summation of the reached fractions of the critical discrete value of the different field frequency bands. So if for example two field frequency bands are present, for each one the fraction of the maximum allowed field strength has to be determined and both fractions are added. The criterion is labeled as a "criterion for different field sources", but also has to be applied for one field source that emits fields of different frequencies. The summation criterion makes the measurements of multi-frequency signals according to 26. BImSch rather difficult, as a measurement device must not only separate the different frequency signals and compare them to (potentially different because frequency-dependent) critical values, but also has to do the weighting according to Formula 2. In particular frequency-converter generated voltage and current signals tend to show a broad spectrum of magnetic field frequencies. This fact can be observed in several parts of this publication.

In 26. BImSch no further information about technical aspects of the measurement can be found. For this the
DIN EN 50413 (August 2009) [11] is cited.

The **BGV B11** [8] is a guideline released by the former "Maschinenbau und Metall-Berufsgenossenschaft". This organization was responsible for the prevention of accidents in the working environment and also for financial compensation and rehabilitation of victims of accidents and occupational illnesses in the business branches of mechanical engineering (also related sub-branches) and since 2011 is part of the larger employers mutual insurance association "Berufsgenossenschaft Holz und Metall" (BGHM).

The BGV B11 guideline obliges enterprisers to measure magnetic fields, to document the measurements, to mark contaminated areas and in the case of a potential harm to limit the access to the contaminated areas. Expositions are classified into four levels:

- Exposition Area 2 is the most harmless classification. All areas belong to this classification, unless their magnetic field contamination exceeds the criterion limit.
- Exposition Area 1 reflects a slightly increased magnetic field contamination. As long as the exposition is limited to regular working-day-periods, no further measures have to be undertaken. By notifying the workers to exercise care and by the time limit of one working-shift the area is then treated as non-critical.
- Areas of Enhanced Exposition ("Bereich erhöhter Exposition") represent a significant increase in the magnetic field. Access to these areas has to be limited to 2 hours per working day and precautions have to be undertaken to avoid further contamination.
- Danger Area ("Gefahrenbereich") must be inaccessible during the periods of magnetic field contamination. This usually involves structural barriers.

In BGV B11 a sum-up of different field frequency bands which contribute to the total magnetic field contamination is only mandatory if field frequencies above 29 kHz are present.

As an example the critical values for a 50 Hz magnetic field (as it is discussed in Section V (C) of this publication for a distribution transformer) has to be below 242 µT to be in Exposition Area 2, below 1,258 mT to be in Exposition Area 1 and below 2,546 mT to be still within the Area of Enhanced Exposition. A magnetic flux density higher than 2,546 mT would result in a Danger Area and would force the owner of the transformer to prohibit the access.

It is noteworthy to mention that the limits given for Areas of Enhanced Exposition and Exposition Area 1 are given for the "full body". If only extremities can reach the contaminated area, 2.5 times the contamination levels are permitted. The BGV B11 also states clearly that this regulation is only to be applied if 26. BImSch cannot be applied. This usually requires a thorough study of the terms and conditions for both regulations.

Both guidelines [8] and [9] also regulate on electric fields, which are not covered by the review in this passage.

Apart from national and international guidelines several companies and organizations oblige their own R&D departments and external manufacturers to uphold certain specific magnetic field criteria. Examples for companies with own guidelines can be found in security-related business branches like in military and in aeronautics, but also in companies which are in public perception like automotive and medicine.

V. MAGNETIC FIELDS IN THE VICINITY OF HIGH-VOLTAGE POWER LINES

All western countries rely on a more or less dense network of high-voltage and highest voltage power lines to connect power plants to the consumer industry and households. In Germany the construction of new power lines is discussed highly controversially. Local resident protests and political constraints aim to delay or prevent the construction. However it is accepted as a necessity by many to increase the transport capabilities for electric energy from the North- and East Sea and the low mountain ranges in northern and middle Germany to the industry centers in the south and west to further pursuit the exit from nuclear and fossil fuel energy [12].
Apart from ambiance misshape and nature protection the protests often focus on the magnetic field contamination near the power lines. Within this publication several measurements have been conducted to analyze the field contamination in the vicinity of:

(A) 380 kV power line
(B) 110 kV power line
(C) transformer substation in industrial estate

For all measurements the MFA-110 was chosen as the measurement device with highest signal amplification and with a standard detector head of 100 cm^2, to fulfill the requirements of most measurement standards. The measured magnetic fields have been compared to the German 26. BImSchV [9], also the magnetic flux density amplitude values have been analyzed separately.

Fig. 4: Measurement sites: *380 kV and 110 kV power lines*

(A) Measurements near a 380 kV power line

The chosen power line is part of the German north-south power-connection and already in use since more than 20 years. Its three-level structure carries in total 12 cable bunches with quadrupole topology (compare Fig. 4).
The measurements have been conducted around 08:00 local time, which is known to be within the timespan of the highest industrial power demand [12]. The measurement positions were at ground level, starting from the symmetry axis of the electrical tower with increasing distance away from it, up to 80 m (Fig. 5 left side). The minimum distance to the cables was around 20 m (directly underneath).

At the center position the voltage signals have been monitored (Fig. 6). The induced voltages for all three measurement coils in the detector head are shown, they correspond directly to the magnetic field strength and frequency. As the orientation of the measurement head was not fixed relative to the power line position, all three perpendicular coils contribute to the total magnetic field signal.

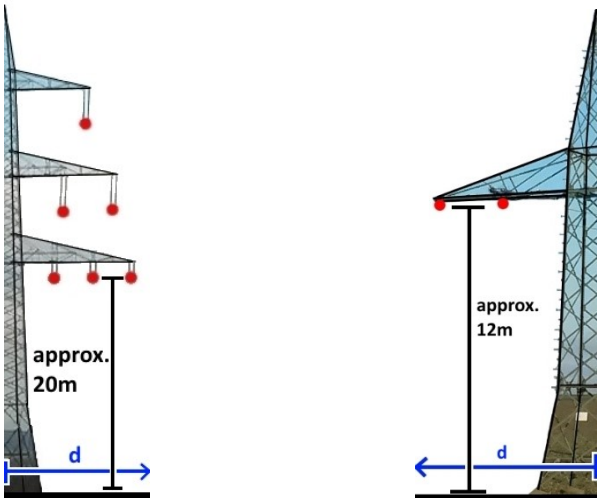

Fig. 5: (left side): *Measurement position explanation 380 kV power line;* ***(right side)****: Measurement position explanation 110 kV power line*

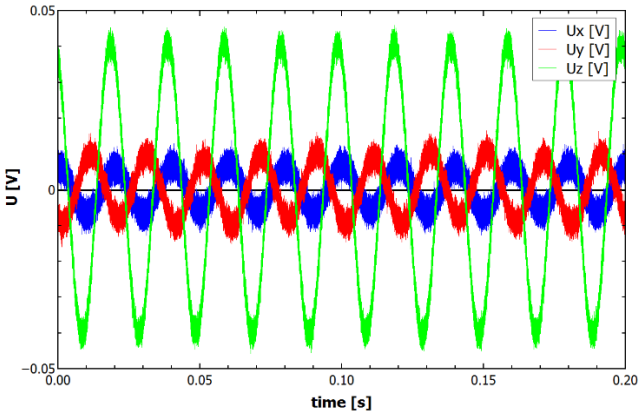

Fig. 6: *Measured voltage signals at center position.*

The shape of the measured signals indicates that the measurements were at the lower range of the possible detector sensitivity. A considerable signal distortion due to internal voltage noises is present. Nevertheless the magnetic fields are still measurable.
Fig. 7 shows the frequency dependent magnetic flux densities (absolute value) signal analysis obtained by the MFA-110-internal FFT, both logarithmic and linear.

The noise at the voltage signals in Fig. 6 result in magnetic flux density noise signals in the logarithmic plot with an intensity of up to 10 % of the dominant 50 Hz signal (compare to the linear scale in Fig. 7). For other measurement points with larger distance to the cable bundles the noise intensity is up to 30 % of the 50 Hz signal intensity. In contrast to other measurements in this publication, no harmonic frequencies seem to be present. This is not surprising, as to our best knowledge the probed power line is not directly connected to a power inverter, but to high voltage transformers on both sides.

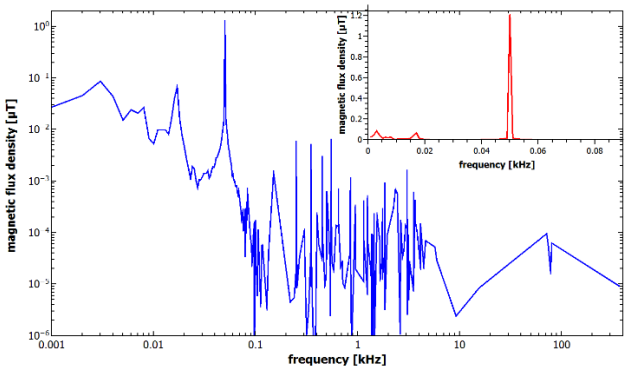

Fig. 7: *Frequency distribution of the measured magnetic flux densities (RMS) in logarithmic (main plot) and linear scale (inlay).*

The measured magnetic flux densities are plotted depending on the distance on ground in Fig. 8. Directly underneath the cable bundles the field amplitudes reach their maximum values. With increasing distance to the cables the intensity is reduced. It is noteworthy to mention that the distance indication on the ground is not the distance r to the lowest cables, but the d-coordinate on the ground (Fig. 5).

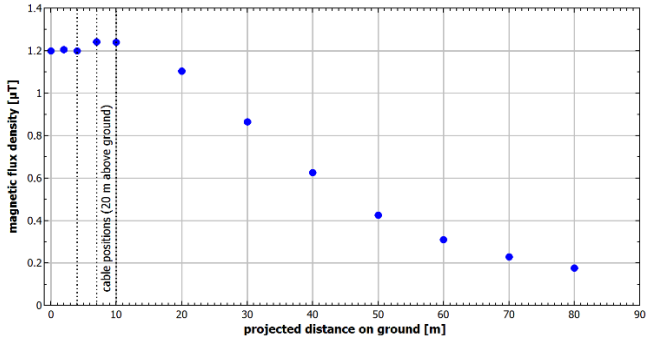

Fig. 8: *Magnetic flux density (at highest intensity, RMS) in dependence of the projected distance on ground of a 380 kV power line.*

Analysis of the magnetic field dependence on the air-line distance can be performed and is shown in Fig. 9. In contrast to the Biot Savart law (Formula 3), which predicts a linear decrease in the field amplitude with the distance, the behavior is not strictly linear. Even in a more complex model, where the resulting magnetic field strength at a given place is composed by the superposition of the fields of the up to 12 cables with the three different phases, the behavior still is expected to be linear, as all current flow directions are parallel.

$$|\vec{B}| = \frac{\mu_0}{4\pi} IR \int_{-\infty}^{\infty} \frac{dl}{(R^2 + l^2)^{3/2}} = \frac{\mu_0}{2\pi} \frac{I}{R}$$

Formula 3: *Biot Savart law for a long wire depending on current I and in-air distance to current R [13].*

There are several possible explanations for the nonlinear behavior: It is difficult to determine the exact orthogonal distance to the power line without the help of geographical survey equipment. An angular error in the measurement line d could falsify the linearity. Another explanation could be the decreasing signal intensity with the distance. Compared with the measurement ranges of the MFA-110 in Table 1 the measured intensities are at the lower end. Also it is still possible that an unknown influence of for example underground power lines in the area is present.

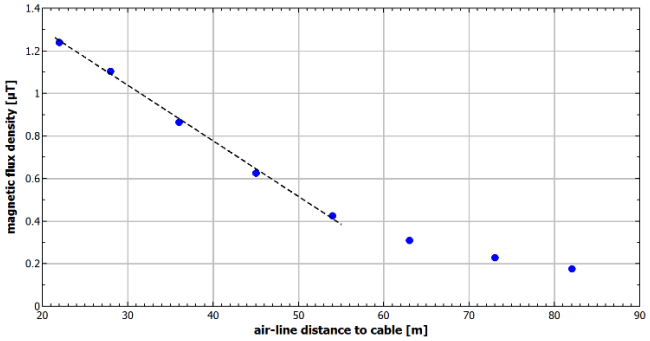

Fig. 9: *Magnetic field strength (at highest intensity, RMS) in dependence of the air-line distance of a 380 kV power line.*

Compared to the guideline 26. BImSchV [9] the measured magnetic fields were below 2 % of the allowed field contamination for all distances.

(B) Measurements near a 110 kV power line

The measurement was conducted near an electrical tower that was unusually close to the ground level. The voltage signal behavior was similar to the one shown in Fig. 6. The FFT analysis also showed a dominant signal at 50 Hz and a quite comparable noise level to (A). Measurements were only possible to a ground-distance of 30 m due to a street in the vicinity.

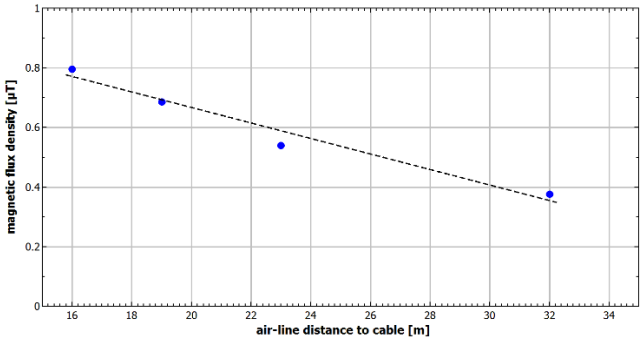

Fig. 10: *Magnetic flux density (at highest intensity, RMS) in dependence of the air-line distance of a 110 kV power line.*

It is noteworthy to mention that in Fig. 9 as well as in the here presented Fig. 10 a linear behavior can be assumed in the range starting from the most outward current-conducting wire to the place where the magnetic field strength drops to 0,4 µT.

The magnetic field pollution in the area under and beneath the power line cables were evaluated according to the guideline 26. BImSchV [9] and where <1,6% of the allowed field intensity.

Better results in both measurements (A) and (B) would be achievable by exact knowledge of all relevant distances and by the use of a project-specific detector head with a better sensitivity in the low-intensity range. Knowledge of the relevant frequency and intensity ranges enable to wind induction coils with different winding numbers and cross-sections. This detector head will not be suitable for guideline measurements like [6], [7], [8] or [9], but allow a more exact measurement of the

50 Hz low intensity field. As already noted the measurements do not contain any information about the electric field.

(C) Measurements at transformer substation in an industrial estate

Since the establishment of inverter technology in many aspects of human life and work, sustainment of power quality is a widely discussed topic [14], [15], [16]. In particular industrial areas are suffering from a high density of drive systems in e. g. CNC lathes and automated storage systems and also from thyristor-controlled power output for example in heating processes. The international EMC norms (e. g. [17]) acknowledge these differences in environmental conditions and define classes of magnetic environments. For industrial devices these classes are usually either class 3 or 4 ([18]). These devices do not need to fulfil the more strict EMC compliance rules of household devices ([19]), but must also be able to withstand a higher noise level.

Within this publication measurements of the magnetic field emission of a transformer station (Fig. 11) in an industrial area are presented. The measurements were done to document the field strength distribution around the building as well as to analyze the power quality without the need to access the building or to apply a direct electrical contact to the transformers.

The time-dependent magnetic field strength was acquired at the backside of the transformer station and is presented in Fig. 12. The signal shows a non-sinusoidal behavior with a high content of harmonics. In Fig. 13 signals at multiples of the dominant 50 Hz mains frequency can be observed. The relative amplitudes of the fundamental frequency and of the harmonics are given in Table 2. Odd numbered harmonics dominate the FFT analysis spectrum, while even numbered harmonics are hardly to detect.

Fig. 11: *Measurement site: Transformer station in an industrial estate.*

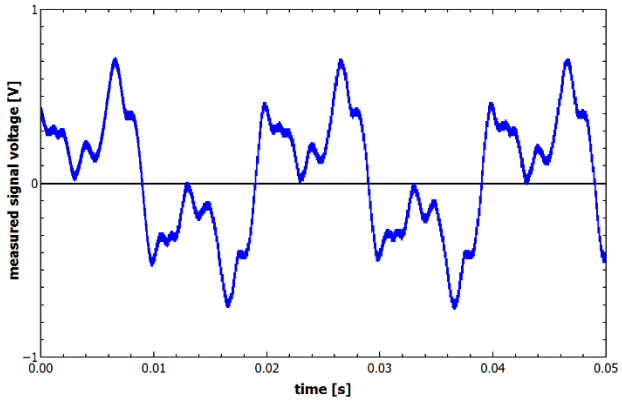

Fig. 12: *Measured voltage signal at the back of the transformer station*

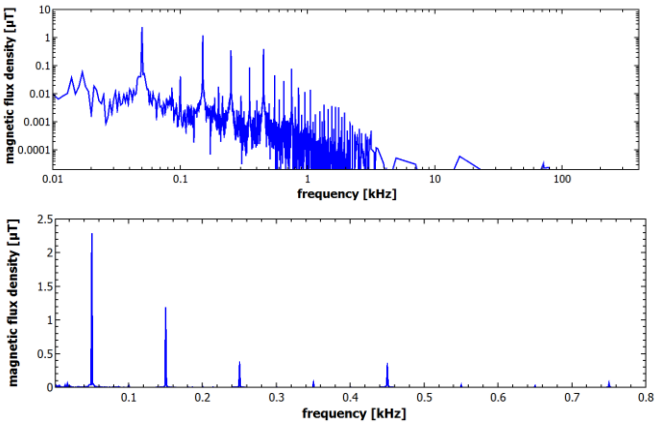

Fig. 13: *Logarithmic (top) and linear (bottom) magnetic field FFT at the transformer station backside (both RMS).*

frequency [Hz]	harmonic No.	abs. intensity [µT]	rel. intensity [a.U.]
50	**1**	**2,3**	**1,000**
100	2	0,03	0,013
150	3	1,15	0,500
200	4	0,012	0,005
250	5	0,32	0,139
300	6	0,007	0,003
350	7	0,07	0,030
400	8	0,004	0,002
450	9	0,31	0,135
500	10	0,003	0,001
550	11	0,03	0,013
600	12	0,004	0,002

Table 2: *Relative and absolute intensities of the measured fundamental frequency and harmonics.*

The THD (total harmonic distortion) is defined as the ratio of the summed power in all harmonics and the power of the fundamental frequency. As no direct access to the transformer was possible and as a result no direct power information is

available, it was only possible to determine the "magnetic field M-THD".

$$\mathrm{THD}_{\%} := \frac{\sum \mathrm{P_h}}{\mathrm{P_f}} \cdot 100\% = \frac{\mathrm{P_{h1}} + \mathrm{P_{h2}} + \cdots + \mathrm{P_{hn}}}{\mathrm{P_f}} \cdot 100\%$$

Formula 4: Definition of the total harmonic distortion according to *[20]*.

As the THD is a power-based measure, the M-THD should be defined as in Formula 5:

$$\mathrm{MTHD} := \frac{\sum \overrightarrow{|\mathrm{B}|_\mathrm{h}}^2}{\overrightarrow{|\mathrm{B}|_\mathrm{f}}^2} = \frac{\overrightarrow{|\mathrm{B}|_{\mathrm{h1}}}^2 + \overrightarrow{|\mathrm{B}|_{\mathrm{h2}}}^2 + \cdots + \overrightarrow{|\mathrm{B}|_{\mathrm{hn}}}^2}{\overrightarrow{|\mathrm{B}|_\mathrm{f}}^2}$$

Formula 5: Definition proposal of the M-THD for the analysis of magnetic fields emitted by power electronics.

Using this definition and the measurement values in Table 2 the M-THD of the transformer field can be determined to 1,289. The direct connection of THD and M-THD might prove as an interesting topic for future publications.

The distance-dependent measurement of the magnetic field strength behind the transformer station is presented in Fig. 14 and in contrast to the measurements done at the 380 kV and 110 kV power lines (Fig. 9 and Fig. 10) shows a much faster decay with increasing distance.

The reason for this behavior is presumably that the copper windings in the transformer emit a field in form of a complex multi-pole geometry. Fitting suggests to assume the decay to be exponential (with the coefficients a=2; b=-1,11; assuming that measured values below 0,35 µT are neglected due to a relatively high noise/signal ratio). This suggests that the field decay behavior is much more difficult to understand than the field of a magnetic dipole.

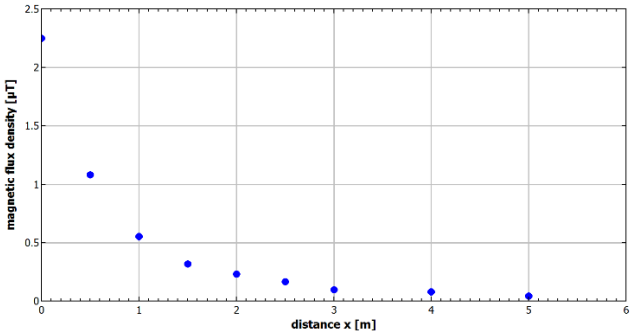

Fig. 14: *Magnetic flux density in dependence of the distance to the transformer station (back side) in RMS.*

For safety reasons the possibility to do area-wide measurements is also important. Systematic execution allows to determine and mark safety-restricted areas. For the transformer station the measurements have been conducted directly around the building, with a distance of 100 mm to the wall. The measured segments where 1x1 m in the front and back area and 1x1,7 m at the sides. In Fig. 15 the magnetic field contamination is displayed color-coded, where green colors indicate low fields while yellow, orange and red indicates stronger fields.

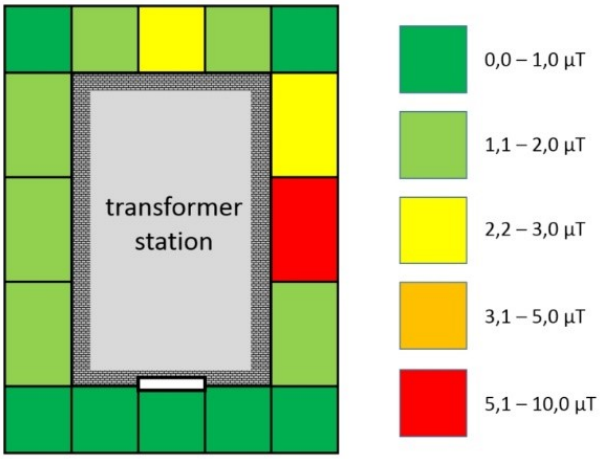

Fig. 15: *Magnetic flux density contamination in the surrounding of the transformer station (RMS).*

In all sections the measured values were considerably below the safety restriction critical values [8] and [9], so that no restriction for the access by the general public is necessary around the transformer station.

VI. OPERATIONAL SAFETY FOR INDUCTION HEATING SYSTEMS

In most electro-technical applications (e. g. motors, transformers, chokes) the induction of eddy currents into a conductive object is an unwanted effect, as it increases the losses of the component and reduces its efficiency. In inductive heating processes this eddy current induction has a beneficial use. Induction heating is a very versatile approach that can be used in a wide field. Mostly it is applied to heat up a system for either thermal relaxation (wires, rods, profiles, e. g.), hardening (drive shafts, cog wheels, tools, e. g.) or shrinking processes (motor lamination packages). The most prominent advantage of inductive heating in comparison to conventional oven heating is that the field is induced locally, thus reducing process losses and protecting from unwanted heating of neighbor structures. Depending on the volume of the object, the inductive heating process is a rather quick and space-saving process for assembly lines.

For inductive heating different frequencies are used, mostly between 1 kHz and 1 MHz. This is a region that is already acknowledged to be potentially harmful in most safety guidelines. To introduce a sufficient thermal heat into the work piece, the intensities of the magnetic fields are usually rather strong. As a result for most inductive heating devices the fulfilment of safety guidelines is a critical issue and shielding of induction machines is important.

Within this publication measurements conducted at an inductive wire heating machine (Fig. 16) are presented. The measurements have been conducted at a frequency converter frequency of 3 kHz and 50 % of nominal power. The machine is shielded by a steel plating box, measurements in the interior of the box were not possible.

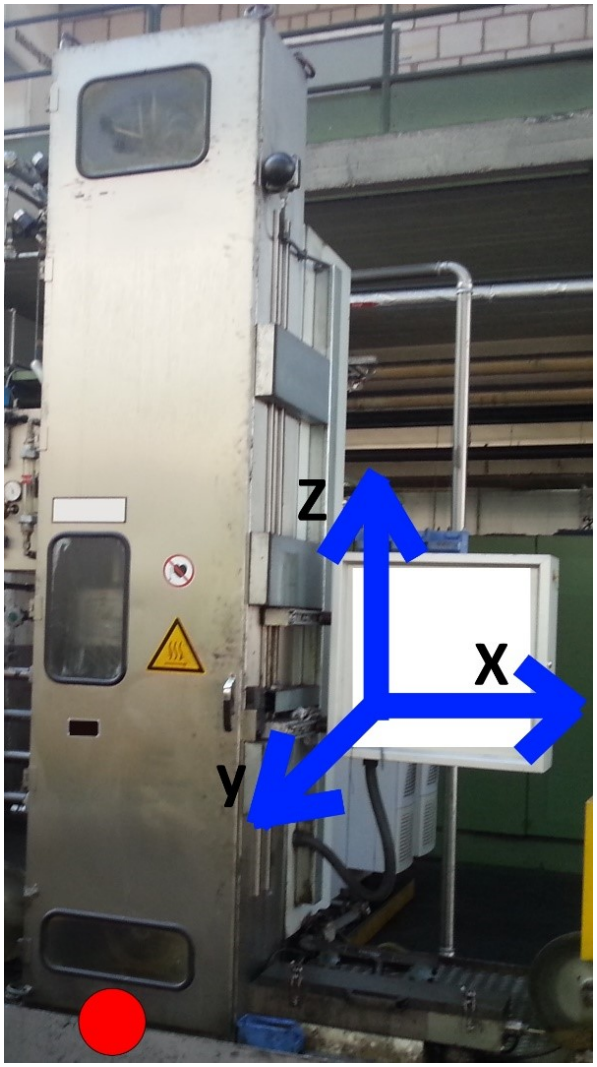

Fig. 16: *Measurement site: Inductive wire heating machine with coordinate system axes (blue) and zero point (0;0;0) (red dot).*

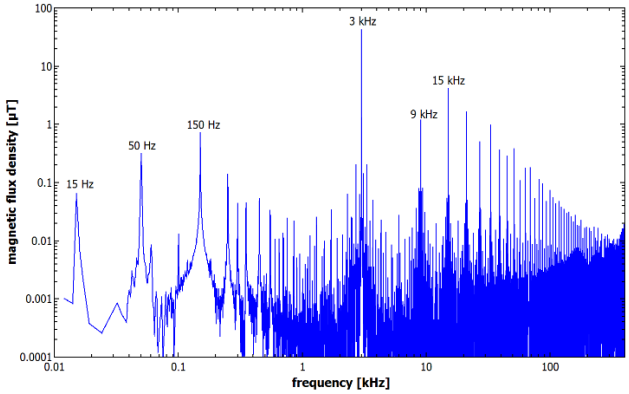

Fig. 17: *Frequency dependent magnetic field analysis of inductor at maximum field strength in log/log (RMS).*

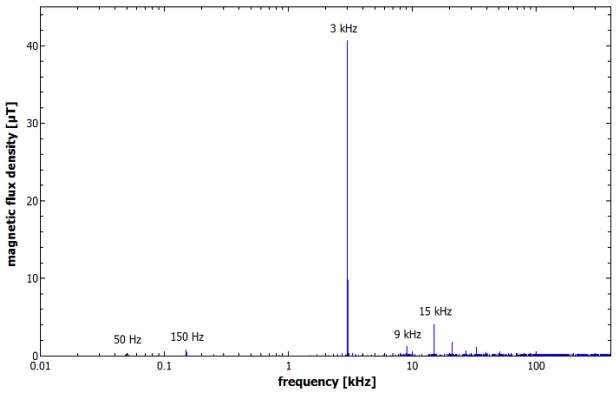

Fig. 18: *Frequency dependent magnetic field analysis of an inductor at maximum field strength in log/lin (RMS).*

Fig. 17 and

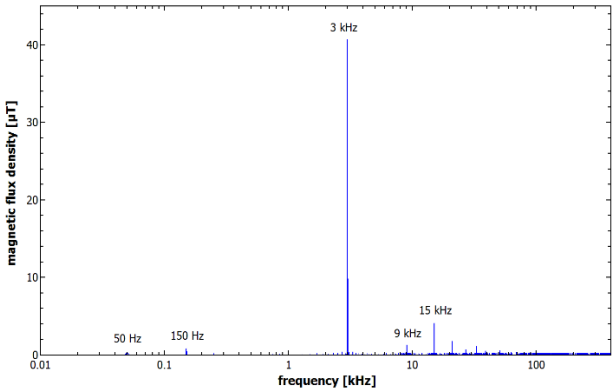

Fig. 18 show the magnetic flux densities at the highest intensity point of all conducted measurement series. In both plots several frequencies can be observed: low-frequency fields (15 Hz, 50 Hz and 150 Hz) and also fields in the kHz range (3 kHz, 9 kHz, 15 kHz, …). The 3 kHz peak can be identified as the induction machines primary frequency, the higher frequencies are odd multiples of this frequency (higher order harmonics). The low frequencies are suspected to be from the machine's mains. This issue will be discussed later in this publication.

The important aspect of the measurements for the manufacturer of the system as well as for the user was the magnetic field pollution in the surrounding area and the possible necessity according to BGV B11 [8] to mark or even barricade a certain area while the machine is working. For applying the BGV B11 laws it is important to know which field frequencies are present, because the critical values are frequency depending. Also for frequencies >29 kHz a summation of the different frequency field contributions is demanded.

For the induction heating machine the analysis is simplified, because the magnetic field pollution is mainly caused by one defined field frequency at 3 kHz. A rough estimation of the energy density (by numerical integration of the area below the magnetic field curves) shows that more than 98 % of the totally emitted energy can be attributed to the 3 kHz signal. Also no significant fields at frequencies above 29 kHz are present. So it is not necessary to do a summation, a comparison of the 3 kHz-field intensity with the critical value at 3 kHz will be sufficient.

In Fig. 19 and Fig. 20 measurements of the magnetic flux density at different positions are shown. Fig. 19 shows a variation of the Y-coordinate for three different heights above ground (Z-coordinate), while Fig. 20 shows measurements at a defined height and distance with different X-coordinates.

The magnetic flux densities are below the critical values for an "Area of Enhanced Exposition", which would be at 67,9 µT and significantly below the critical values for a "Danger Area", which would be present if magnetic flux densities would exceed 127,3 µT. Nearly the whole area around the induction machine is an "Exposition Area 2", while only in <20 cm distance in front of the machine the "Exposition Area 1" limits are reached. As mentioned before, the nominal power of the induction machine can be the double of the parameter that was set up for the measurements. So probably the "Exposition Area 1" will be larger then. However from the conducted measurements it can be concluded that the "enhanced field strength" area will be only within the shielded case of the induction machine. For a documented measurement according to [8] the maximum power output of the machine would have to be chosen, which would not only be a maximum input power, but also the inductor setup and the wire type and diameter with the highest field emission.

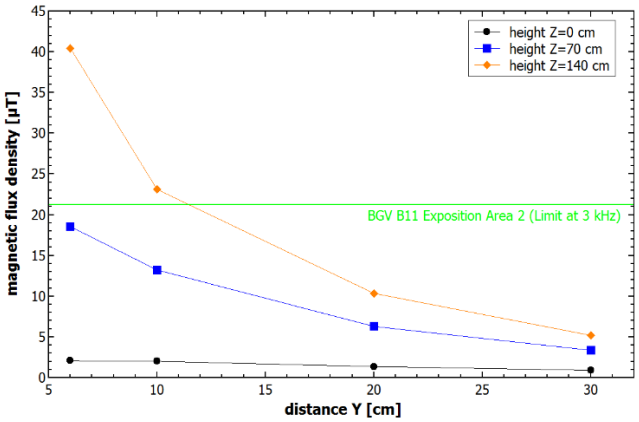

Fig. 19: *Magnetic field strength with increased Y-distance from the induction machine (RMS). Critical value of BGV B11 at 3 kHz is marked green.*

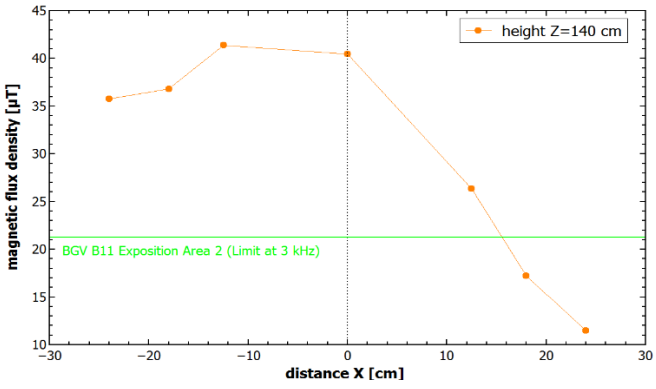

Fig. 20: *Magnetic field strength from left to right (varied X-coordinate) in front of the induction machine (RMS). Critical value of BGV B11 at 3 kHz is marked green.*

Fig. 20 shows that the magnetic field distribution in front of the induction machine is not symmetric with respect to the center of the X-axis. This can be attributed to two reasons: First the induction machine shielding has a window just below (with respect to Z-axis) the measurement point. Also the induction machine is not symmetric in its internal construction. A slope of wire acts as the primary field source, but is influenced by soft-magnetic inductor parts in the area for X>0. These soft-magnetic parts provide an additional shielding, leading to a reduced field for X>0.

The distance-depending measurements can also be used to further analyze the magnetic field at different peak frequencies. This is done in Fig. 21: for different distances the intensity of the different peak frequencies from Fig. 19 are compared.

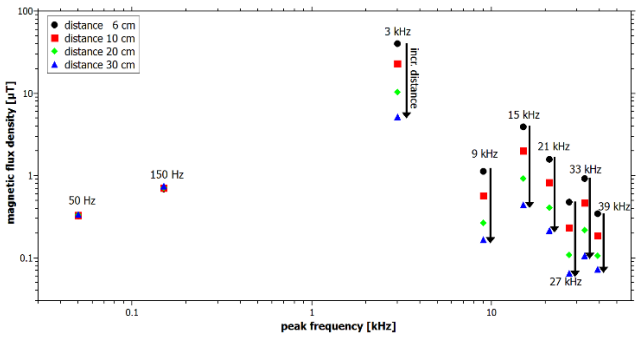

Fig. 21: *Intensity comparison of the peak frequencies from Fig. 19 at different distances to the induction machine.*

All field maxima at 3 kHz or higher behave similarly: the intensity drops remarkably with increasing distance to the induction machine. For the low frequency peaks (displayed here: 50 Hz and 150 Hz) there is hardly any change in the field strength. Our conclusion for this behavior is that the source of the low frequency fields does not lie within the inductor, but possibly in the power supply of the induction machine or in the electric grid of the factory. This information is of interest in particular for consideration of possible shielding measures. For the total field contamination calculation according to [8] they also have to be compared to the critical values and in [9] they even would have to be included in the summation of the total field contamination, nevertheless the origin of this field is not the induction machine.

If the detector head axes are kept parallel to the axes of the measurement coordinate system it is also possible to conduct a vector analysis of the measured field. In the sketches Fig. 22, Fig. 23 and Fig. 24 the directions of the magnetic field vectors have been evaluated and noted. All indicator arrows are normalized to the same length, for a better visual accessibility. The color codes (green: < 5µT; orange > 5µT and < 10µT; red: > 10µT) indicate the field strengths at the respective positions. The field vectors have been found to be in agreement with the internal setup of the induction machine, which in a first order approximation behaves like a magnetic dipole.

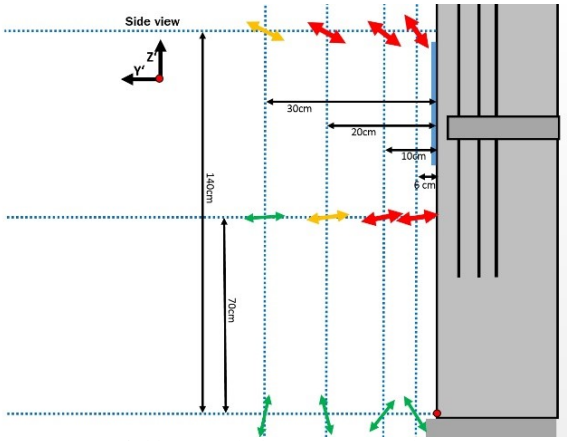

Fig. 22: *Magnetic field vectors (side-view projection).*

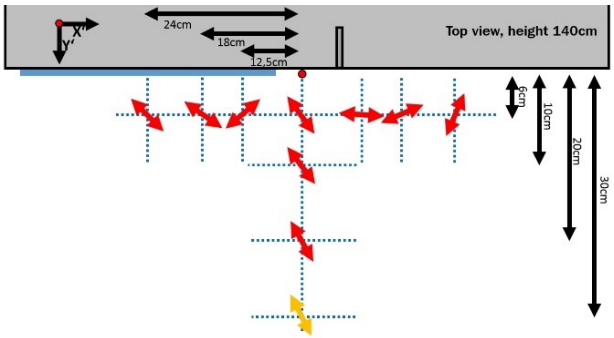

Fig. 23: *Magnetic field vectors (top-view projection).*

For further analysis and comparison with external parameters the MFA-110 features a fourth channel, which can be used to monitor an external voltage signal. This channel has been used to capture the primary inductor current with a current clamp. In Fig. 25 this inductor current is presented together with the voltages that have been induced in the MFA-110 (calculated to absolute voltage values). The fundamental frequency of both signals is the same, but there is a significant difference in the measured signal.

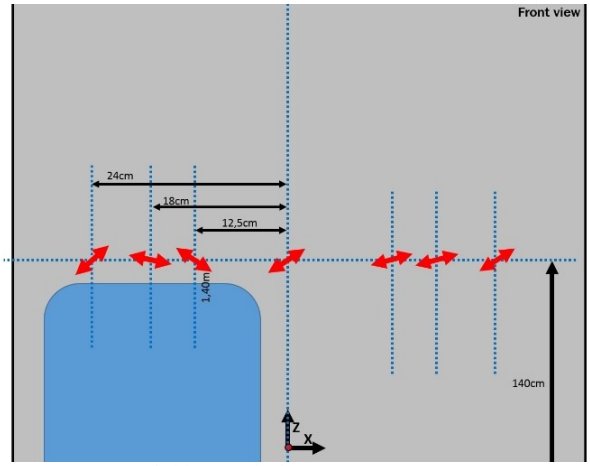

Fig. 24: *Magnetic field strength (front-view projection).*

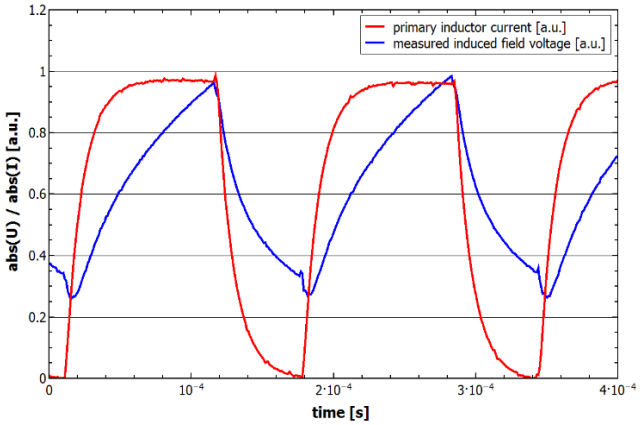

Fig. 25: *Primary inductor current and measured induced voltages (by MFA-110).*

A suitable explanation for this difference might be the interpretation of the inductor components (internal soft-magnetic parts as well as magnetic shielding) as a "general" inductive component. For both curves the signal increments behave according to an exponential function with a time constant $\tau=L/R$ (fits not shown here). For the "undamped" signal (primary inductor current) the ratio of L/R would be 12 µs, for the "damped" signal (measured magnetic flux density) it would be around 62 µs.

VII. MAGNETIC FIELD MEASUREMENTS IN MOTOR CIRCUITS

Modern drive circuits are known to be a major source of electromagnetic disturbances [21], wire based in the energy supply grid as well as field-driven in neighboring circuits and in the surrounding environment. Disturbing voltage noise transmission to the power supply grid can be reduced by a sufficient output filtering. This is in particular of importance for regenerative drives, which redirect non-neglectable amounts of energy back to the power supply grid. But also in the drive circuit itself sufficient filtering is of importance. Frequency converters provide motors with a voltage of variable frequency formed by IGBT or other semiconductor devices. The voltages are generated by more or less sophisticated switching procedures, opening and closing the semiconductor valves cyclically. The voltages applied to the motor are of non-sinusoidal (mostly rectangular) shape, consisting of a broad variety of harmonic frequencies. These frequencies are a source of additional losses in electrical machines, because hysteresis losses increase linearly and eddy current losses even quadratic with the exciting magnetic field frequency [22]. "Better" switching techniques, like pulse duration modulation can reduce the content of harmonics in the circuit and the effective current is also smoothened by the motor winding inductance. But in many drive circuits additional filtering by e. g. a motor choke is necessary.
The switching of the IGBT valves occurs rather fast, forming high voltage gradients. These gradients, in combination with long motor cables, can damage motor insulation layers, increase motor aging and are one of the sources of motor bearing currents [23]. Using dU/dt-filters [24] often is a suitable measure to smoothen the voltage flanks. These filters are in particular of importance when old motors which often have weaker insulation and are not suited for frequency converter use, are used as a variable speed drive.

Noise voltage signals of different origin can be measured directly in the motor circuit, but are also detectable through the magnetic field in the surrounding area. The emitted fields are typically in the lower kHz range and can be detected with magnetic field measurement devices like the MFA-110. In this section of the publication measurements at a drive system are presented and discussed. A setup consisting of a frequency converter and a permanent magnet synchronous motor has been analyzed with respect to the emitted magnetic field frequency spectrum at different rotational speeds. Also magnetic shielding foils made of MUMETALL® and VITROVAC® 6025 X have been used to reduce the magnetic field emittance of frequency converter and motor. The analyzed motor was a permanent magnet synchronous machine with a nominal rotational speed of 4500 1/min. The motor was connected to a 16 kVA frequency converter. Motor and frequency converter are shown in Fig. 26 and Fig. 27. They were connected by conventional three phase non-shielded litz-wire with a length of 1m.
Both components were chosen, because they represent a typical small industrial application synchronous motor which could be used in plant construction tasks.

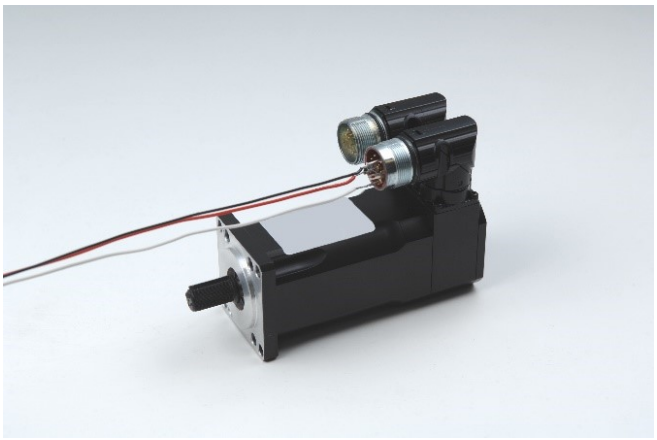

Fig. 26: *Permanent magnet synchronous motor with unshielded litz wire connection used in measurements.*

Strong magnetic fields are expected during the starting and acceleration phases of motors, as not only power is introduced into the system to compensate friction, but also to accelerate the motor (and load).

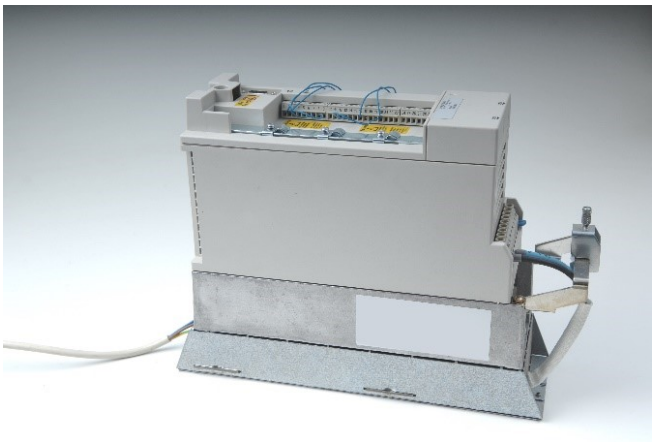

Fig. 27: *1,6k VA Frequency converter used in measurements.*

In Fig. 28 measurements of the magnetic field directly at the motor are shown in dependence of the field frequency. The measurements have been conducted for a total measurement time of 30 seconds in the acceleration phase of the motor. At the beginning of the measurements the motor is resting and without current, at the end it has reached its nominal rotational speed.

The measured data are accumulated in measurement frames, each consisting of a 2,5 s timespan. This timespan is only an auxiliary tool and its length can be changed at any time, even after the measurement. Its purpose is to limit the amount of calculation effort for a specific measurement segment and also to provide a suitable sectioning mechanism for time-dependent signals. The chosen timespan however sets a limit to the lowest field frequency that can be determined by the Fourier transformation. In Fig. 28 the measured magnetic field is shown over the full 30 seconds timespan. The signals of different frames are color-coded and it can be observed that the frequency changes with increasing time from a maximum at 50 Hz to 400 Hz. The shape of the curve also changes significantly during this transition.

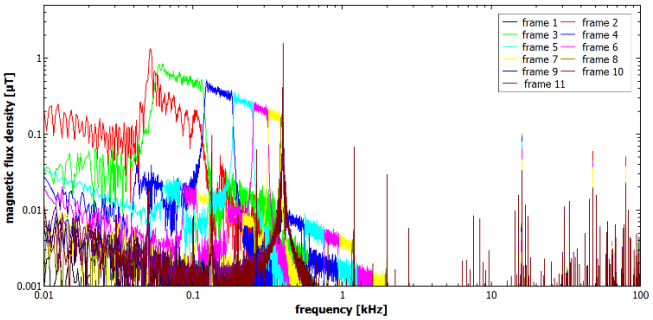

Fig. 28: *Magnetic field at the motor during motor start with a frame length of 2,5 seconds.*

Frequency converters are expected to deliver a voltage with a defined, variable frequency. In Fig. 28 however the shape of the frequencies seems to have a more block-like shape. The reason for this is that a frame in Fig. 28 consists of measured signals over a time of 2,5 seconds each. So the measured magnetic field is a superposition of the magnetic field frequencies in this time interval. In Fig. 29 the frame size is reduced to 0,25 seconds each, reducing the superposition effect significantly. In Fig. 29 six frames with a length of 0,25 seconds are shown. The measurement was done continuously, but for clarity reasons only every tenth frame is shown. The curve shape now has changed to a defined sharp maximum for each of the measured frames. Now it is obvious that the motor starting sequence contains is a continuous frequency shift from 50 Hz to 400 Hz. This emphasizes that the frame length is a crucial factor for transient analysis.

The process of magnetic field measurement allows to also monitor the voltages which are induced into the three orthogonal detector coils of the MFA-110. They are presented in Fig. 30 and show a 300 Hz primary signal and a higher frequency ripple.

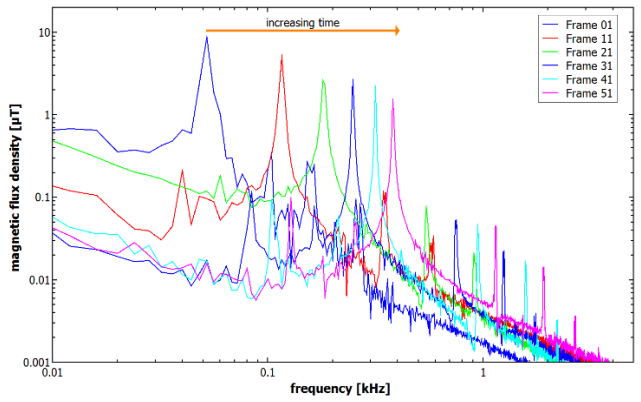

Fig. 29: *Magnetic field at the motor during startup with a frame length of 0,25 seconds.*

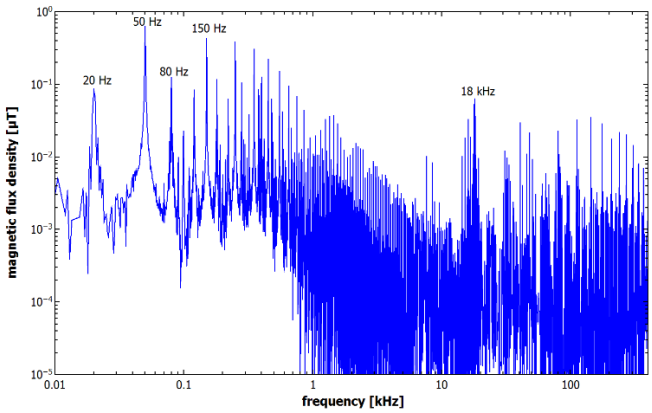

Fig. 32: *Magnetic flux density spectrum measured in "max hold" measuring mode around the frequency converter (RMS).*

Measurements of the magnetic flux density were also conducted around the frequency converter (Fig. 31). Fig. 32 shows results which were obtained by a "max hold" measurement. This measurement mode detects and plots the maximum magnetic flux density for each frequency band within the measurement time. "Max hold" measurements are in particular useful for looking for a "worst case scenario" in a certain area. The measurement was conducted with a 30 seconds timespan with the motor already having reached its nominal rotational speed. The spectrum shows a dominant 50 Hz peak attributed to the power supply part.

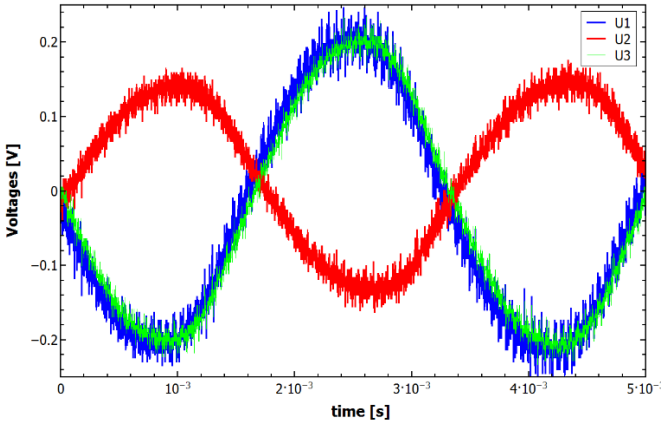

Fig. 30: *Measured voltages (V1, V2, V3) during motor starting phase.*

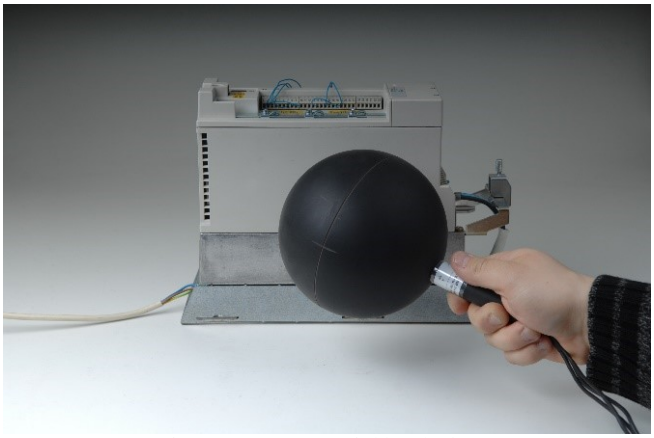

Fig. 31: *Position of maximum magnetic field at the frequency converter.*

The comparably small motor allowed to do extensive tests with different shielding materials and investigations of the shielding factor. The shielding factor according to [25] and [26] is determined by the ratio of the field with and without a shielding (compare Formula 6). It is frequency-dependent, as most shieldings show a strong frequency influence on permeability, saturation and field displacement.

$$S(x,y,z) = \frac{H_{nS}(x,y,z)}{H_S(x,y,z)}$$

Formula 6: Definition of the shielding factor according to [26].

Also the shielding factor is depending on the position in a shielding. This effect is in particular significant, if only a sheet/plate is used, without a stray-field reducing magnetic backflow. More information about magnetic shielding can be found in [25] and [26].
As motor and frequency converter emit magnetic fields in a broad frequency range, it is possible to investigate the frequency dependence of the shielding factor. This was done by measurements with different shielding objects:

a) Foil of MUMETALL® (t= 0.1 mm)
b) Foil of VITROVAC® 6025 X (t≈ 25 µm)
c) Casing of MUMETALL® (folded and closed box, Material as in a)).
d) Copper plate (t= 1 mm)

The first approach was to analyze the maximum peak values at the nominal rotation speed of the motor and to calculate the shielding factor at these defined frequency values. The detector head was fixed in a distance of 3 cm to the motor, with the shielding in the remaining space in between. Fig. 33 shows the frequency dependent magnetic fields for the different shielding case studies.

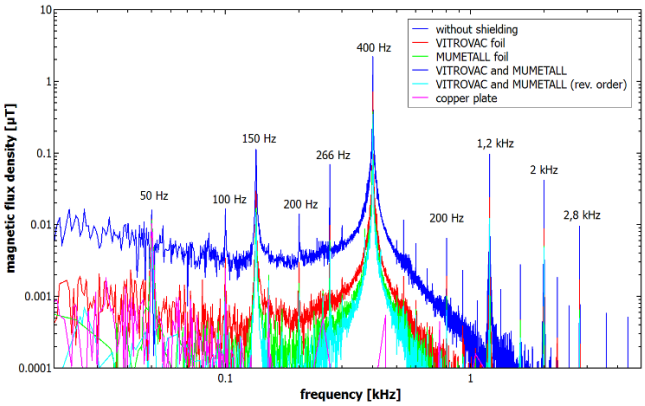

Fig. 33: *Magnetic flux densities (RMS) compared for different shielding measures (motor at nominal rotational speed).*

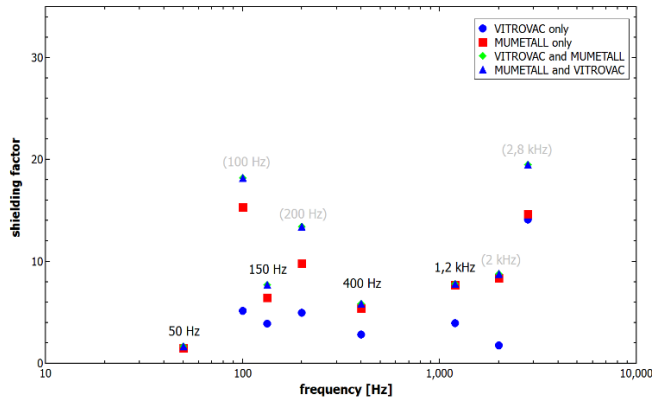

Fig. 34: *Shielding factor determination of the different shielding measures at nominal rotational speed from Fig. 33. Unreliable low-intensity measurement points are marked in grey.*

It became obvious that the evaluation of the shielding factor had a large error, for two reasons: On one hand the stationary motor condition does not provide a maximum strength field. The motor starting phase would produce larger fields. Also the peaks are very sharp and narrow, so it is possible that their measured intensities are distributed between two neighboring frequency intervals, thus reducing the effectively measured maximum peak value. The deviations led to shielding factors with a large deviation (Fig. 34) by the frequency. This is not only unexpected, but also does not suit to theoretical expectations.

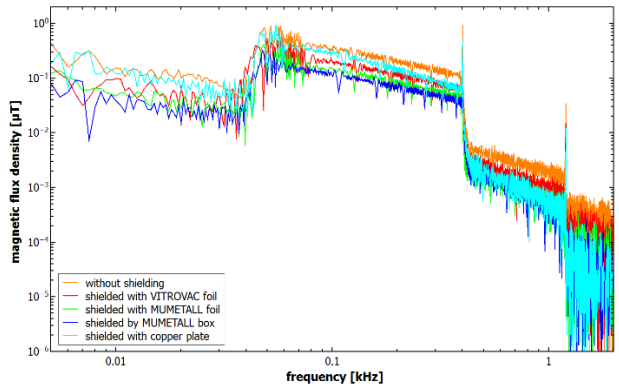

Fig. 35: *Magnetic flux density (RMS) for different shielding measures during the motor starting phase.*

Much better results were achieved by analyzing a broad-band part of the motor acceleration spectrum. In Fig. 35 several decaying-plateau-like structures can be recognized, which proved to be suitable for analysis. Fig. 36 and Fig. 37 show these sections in a magnified view and with a linear frequency scale. Fitting with exponential decay curves and dividing the curves as in Formula 6 led to the shielding factor curves in Fig. 38. Compared to Fig. 34 the resulting curves seem to be much smoother and lie within the expected shielding factor range of $S \approx 2\text{-}5$.

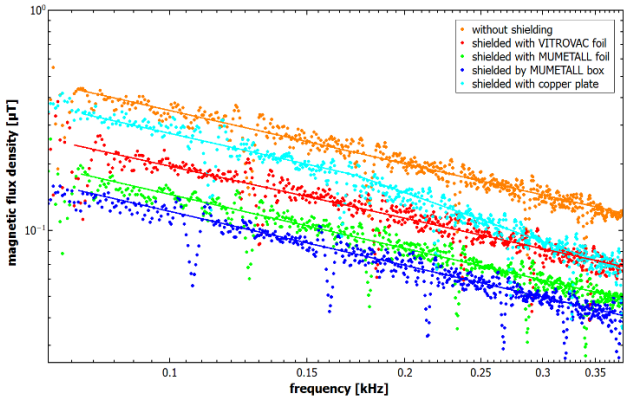

Fig. 36: *First analysis region for shielding factor determination from Fig. 35 (all flux densities in RMS).*

Noteworthy details of this investigations are that it can be recognized from the measurements in Fig. 36 and Fig. 37, that an increasing frequency also increases the shielding effect of the copper plate. Copper does not show ferromagnetic behavior, so its attenuation effect can be neglected for DC fields and increases with increasing frequency. Copper is only able to reduce magnetic fields by supplying movable electrical charges on its surface, which can be set into motion in form of eddy currents. In general, all conductive materials (ferromagnetic or not) show an increasing field displacement effect with increasing frequency, depending on their respective electrical conductivity and relative material permeability [27], [28]. For ferromagnetic material this means a reduction of the magnetic flux conducting cross section. For both types of materials it results in a confinement of the electrical charges beneath the surface of the material.

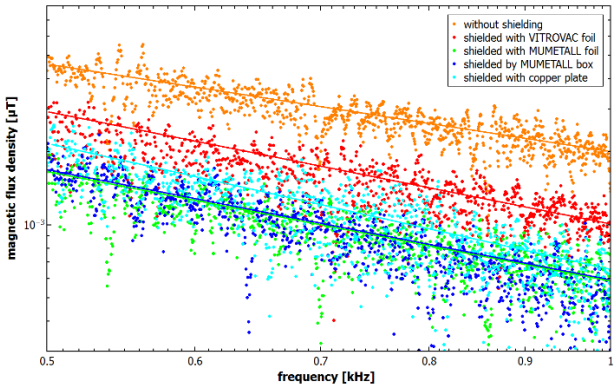

Fig. 37: *Second analysis region for shielding factor determination from Fig. 35. All flux densities are given in RMS.*

The differences in the shielding effects of the MUMETALL®-foil and the MUMETALL®-box are decreasing with increasing frequency. This can be explained by an increase of the eddy-current-related shielding effect, which takes place more localized than the magnetic flux guidance shielding contribution.

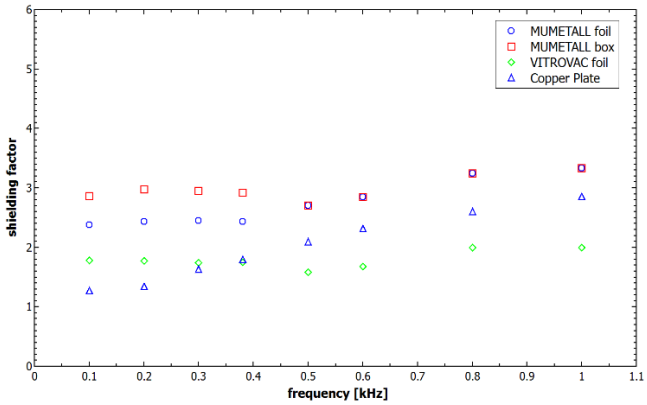

Fig. 38: *Frequency depending shielding factors derived from Fig. 35, Fig. 36 and Fig. 37.*

As a general remark it should be stated that the relatively low shielding factor of the MUMETALL-box can be attributed to the comparably thin material cross section. Permanent magnetic synchronous motors are usually a typical example for rather strong magnetic field sources, in particular in the area directly around the motor. With a closed MUMETALL®-shielding of a sufficient wall thickness for this example motor shielding factors of 50-100 should be possible. Basic details on the estimation of magnetic shielding factors can be found in [29].

VIII. Conclusion and Outlook

The measurements presented in this publication are examples of some very different origins, types and frequencies of magnetic fields, of possible measuring and shielding techniques and of some practical hints for the conduction of post-measurement analysis of the data. It could be demonstrated that a flexible and potent magnetic field measuring device like the MFA-110 can be adapted for very different tasks and challenges, sometimes by hardware changes (for example different detector heads for a modified measurement range), but in many cases just by adapting the data acquisition to the respective task. Guidelines for magnetic field contamination like BGV B11 and 26. BImSch have been discussed to ease their interpretation and to give a more practical access to magnetic field measurements according to them. Further publications are planned which cover measurement examples at additional industrial sites and also give more examples for applying the most common guidelines.

References

[1] S. Tumanski, Handbook of magnetic measurements, CRC Press, 2011.

[2] Y. Zhang, „Second order high temperature superconductiong gradiometers for magnetocardiography in unshielded environmens," *Appl. Phys. Lett.,* pp. 76, 906-908, 2000.

[3] Y. Zhang, „Applications of high temperature SQUIDs," *Appl. Supercond.,* pp. 367-381, 1995.

[4] D. R. Popovic, „Three-Axis Teslameter With Integrated Hall Probe," *IEEE Transactions on insturmentation and measurements,* pp. Vol. 56, No. 4, August 2007.

[5] S. AG, „Datasheet - Fully integrated 3-axis Hall probe 03A," 31 07 2015. [Online]. Available: http://www.senis.ch/docs/default-source/datasheet-hall-probe/fully-integrated-3-axis-hall-probe-03a-for-oem-rev02.pdf?sfvrsn=2. [Zugriff am 31 07 2015].

[6] ICNIRP, „Guidelines for limiting exposure to time-varying electric and magnetic fields (1Hz – 100 kHz)," *Health Physics 99(6),* p. 818-836, 2010.

[7] ICNIRP, „Guidelines for limiting exposure to time-varying electric, magnetic and electromagneticfields (up to 300 GHz)," *Health Physics 74 (4),* pp. 494-522, 1998.

[8] BGVB11(VBG25), „Berufsgenossenschaftliche Vorschrift für Sicherheit und Gesundheit bei der Arbeit," *MMBG Maschinenbau- und Metall-Berufsgenossenschaft,* 2002.

[9] 2. BImSchV, „German environmental law," pp. 2129-8-26, 22 August 2013.

[10] ICNIRP Organization, „ICNIRP Organization Website," [Online]. Available: http://www.icnirp.org/en/about-icnirp/aim-status-history/index.html. [Zugriff am 8 June 2015].

[11] DIN EN 50413, Grundnorm zu Mess- und Berechnungsverfahren der Exposition von Personen in elektrischen, magnetischen und elektromagnetischen Feldern (0 Hz bis 300 GHz), Berlin: Beuth Verlag, 2009.

[12] B. M. Buchholz und Z. Styczynski, Smart Grids – Grundlagen und Technologien der elektrischen Netze der Zukunft, VDE Verlag, 2014.

[13] J. Jackson, Classical Electrodynamics, Wiley, 1999.

[14] R. C. Dugan und M. F. McGranaghan, Electrical Power Systems Quality, McGraw-Hill Professional, 2010.

[15] A. v. Meier, Electronic Power Systems - A conceptual introduction, IEEE Press, Wiley, 2006.

[16] A. Baggini, Handbook of Power Quality, Wiley, 2008.

[17] VDE, Electrical equipment for measurement, control and laboratory use - EMC requirements (VDE 0843-20-1:2013-07), Beuth Verlag, 2013.

[18] A. J. Schwab und W. Kürner, Elektromagnetische Verträglichkeit, Springer, 2007.

[19] VDE, Electromagnetic compatibility - Requirements for household appliances, electric tools and similar apparatus (DIN EN 55014-1:2012-05), Beuth Verlag, 2012.

[20] www.wikipedia.de, „www.wikipedia.de / Definition THD," [Online]. Available: https://de.wikipedia.org/wiki/Total_Harmonic_Distortion. [Zugriff am 04 08 2015].

[21] R. K. J. Petzold, „Nanocrystalline materials in common-mode chokes," *EMC Kompendium 2001,* pp. 148-152, 2000.

[22] G. K. K. Küpfmüller, Theoretische Elektrotechnik und Elektronik, Berlin: Springer, 2000.

[23] ABB, Technical guide No. 5 - Bearing Currents in modern AC Drive Systems, ABB, 2011.

[24] J. Specovius, Grundkurs Leistungselektronik: Bauelemente, Schaltungen und Systeme, Berlin: Springer, 2013.

[25] VAC, Magnetic Shielding, Hanau: Vacuumschmelze GmbH & Co. KG, 1989.

[26] S. H. D. F. D. Sekels, Theory and Praxis of Low Frequency Magnetic Shielding Problems, SEKELS GmbH, 2010.

[27] H. Kaden, Wirbelströme und Schirmung in der Hochfrequenztechnik, Springer Verlag, 2006.

[28] W. R. R. Hilzinger, Magnetic materials, Hanau: VAC, 2013.

[29] SEKELS GmbH, Magnetic Shielding, Ober-Moerlen: SEKELS GmbH, 2013.

[30] K. Heuck, D. Dettmann und D. Schulz, Elektrische Energieversorgung - Erzeugung, Übertragung und Verteilung elektrischer Energie für Studium und Praxis, Springer Verlag, 2013.

[31] A. J. Schwab und W. Kürner, Elektromagnetische Verträglichkeit, Springer Verlag, 2007.

[32] G. B. K. H. A. Toliyat, Handbook of Electric Motors, New York: Marcel Dekker Inc., 2004.